Nanoscale and Microscale Thermophysical Engineering, 12: 228–237, 2008

ISSN: 1556-7265 print / 1556-7273 online
DOI: 10.1080/15567260802183015

Taylor & Francis
Taylor & Francis Group

CARBON NANOTUBE ARRAY THERMAL INTERFACES FOR HIGH-TEMPERATURE SILICON CARBIDE DEVICES

Baratunde A. Cola[1,2], Xianfan Xu[1,2], Timothy S. Fisher[1,2], Michael A. Capano[1,3], and Placidus B. Amama[1]

[1]*Purdue University, Birck Nanotechnology Center, West Lafayette, Indiana, USA*
[2]*Purdue University, School of Mechanical Engineering, West Lafayette, Indiana, USA*
[3]*Purdue University, School of Electrical and Computer Engineering, West Lafayette, Indiana, USA*

Multiwalled carbon nanotube (MWCNT) arrays have been directly synthesized from templated Fe_2O_3 nanoparticles on the C-face of 4H-SiC substrates by microwave plasma chemical vapor deposition (MPCVD), and the room-temperature thermal resistances of SiC-MWCNT-Ag interfaces at 69–345 kPa as well as the thermal resistances of SiC-MWCNT-Ag interfaces up to 250°C (at 69 kPa) have been measured using a photoacoustic technique. The SiC-MWCNT-Ag interfaces with MWCNTs grown on the C-face of SiC achieved thermal resistances less than 10 mm^2 K/W, which is lower than the resistances of MWCNT interfaces grown using the same catalysis and growth methods on the Si-face of SiC and Ti-coated SiC. The thermal resistances of the SiC-MWCNT-Ag interfaces exhibit weak temperature dependence in the measured range, indicating that the interfaces are suitable for high-temperature power electronics applications.

KEY WORDS: carbon nanotube, thermal interface resistance, silicon carbide, high-temperature, photoacoustic

INTRODUCTION

Silicon carbide (SiC) electronic devices have developed such that commercial products are now available. SiC is preferred in high-temperature, high-power, and high-frequency applications because its combination of physical properties enables it to outperform Si under harsh conditions. Under such challenging operating conditions, efficient heat flow through the interface from the die to the heat sink or spreader is paramount, and this study considers the use of carbon nanotube arrays to serve this thermal interface function both at room temperature and near the elevated temperatures anticipated in practical applications. The possibility of achieving a gradient carbon morphology from the SiC/C-face to the C-C lattice is of particular interest and could enhance interfacial heat conduction.

Received 16 February 2008; accepted 5 May 2008.

We gratefully acknowledge funding from the Air Force Research Laboratory. B. A. Cola gratefully acknowledges fellowship support from the Intel Foundation and the Purdue University Graduate School.

Address correspondence to Timothy S. Fisher, Purdue University, Birck Nanotechnology Center, 1205 W. State St., W. Lafayette, IN 47907-2057. E-mail: tsfisher@purdue.edu

NOMENCLATURE

E_g	energy gap, J	n_i	intrinsic concentration of carriers, cm^{-3}
h	Planck constant, J·s	T	temperature, K
k_B	Boltzmann constant, J/K		
N_c	density of states at the conduction band edge, cm^{-3}	**Greek Symbols**	
N_v	density of states at the valence band edge, cm^{-3}	λ	characteristic phonon wave length, m
		υ	sound velocity, m/s

Despite the ability of SiC power devices to operate at elevated temperatures as compared to Si devices, thermal issues remain paramount to their performance. In short, excessive thermal loading of a device diminishes the ability to carry current and may lead to catastrophic failure. When defects are present, breakdown of a device is often accelerated. Recent published results examining how SiC Schottky Barrier diodes (SBD) are influenced by defects have demonstrated that forward and reverse characteristics are sensitive to essentially any defect within the active region of the device [1–4]. Defects that are known to degrade diode characteristics include micropipes, comets, carrots, inclusions, small-angle boundaries, and screw dislocations.

Particularly relevant to high-temperature environments is the bandgap energy of SiC. At room temperature, the bandgap of 4H-SiC (the most attractive SiC polytype for electronic devices) is 3.23 eV [5], compared to a 1.1 eV bandgap for Si. Most practical electronic devices are extrinsically doped (i.e., contain controlled levels of foreign atoms to impart specific electrical characteristics) in the range of 10^{13} to 10^{19} cm^{-3}. Charge carriers in electronic devices can also be generated intrinsically by thermal excitation of electrons from the valence band to the conduction band across the energy bandgap. The intrinsic concentration of carriers (n_i) is given by [6]:

$$n_i = \sqrt{(N_c N_v)} \exp\left(\frac{-E_g}{2k_B T}\right), \tag{1}$$

where E_g is the energy gap and N_C and N_V are the effective density of states at the conduction and valence band edge, respectively. It is evident from Eq. (1) that a threefold increase in the bandgap energy achieved using SiC electronics as compared to Si yields an intrinsic carrier concentration for SiC that is orders of magnitude lower than that for Si. As a result, it is possible to operate SiC devices at temperatures as high as 500–600°C, while Si is generally limited to 125°C.

While the foregoing discussion highlights the advantage of SiC over Si for high-temperature applications, it is still important to maintain the coolest operating conditions possible. The electrical conductivity in SiC depends not only on the quantity of charge carriers but also on the mobility of carriers. As temperature increases, phonon scattering of carriers increases and, in turn, increases the resistance to current flow. Device performance suffers as a consequence, and therefore it is essential to efficiently remove generated heat away from the active regions of SiC devices. Further, while high-temperature operation is an appealing attribute of wide bandgap devices, they must operate reliably in extreme thermal environments and often with simplified, less efficient cooling

technologies. The opportunity to reduce interfacial thermal inefficiencies through the use of CNT arrays considered herein would substantially enhance their reliability and utility.

Previous studies [7–16] have demonstrated that multiwalled carbon nanotube (MWCNT) arrays grown on one side of an interface can achieve room-temperature thermal resistances as low as 7–25 mm^2 K/W, depending on the method of fabrication and array morphology. Using transient optical techniques, Wang et al. [11], Cola et al. [13], and Tong et al. [14] revealed that the interfaces between MWCNTs and their growth substrate and the interfaces established at the free ends of MWCNTs can be significant thermal bottlenecks in MWCNT array interfaces. Therefore, to promote good thermal contact at the MWCNT-growth substrate interface, adhesion layers (e.g., Ti, Mo, or Cr) are often deposited on the substrates before MWCNT fabrication [9–15]. Additionally, Tong et al. [14] demonstrated that the resistance at the MWCNT free ends' interface, which was an order of magnitude higher than the resistance at the MWCNT-growth substrate interface, can be reduced up to an order of magnitude by using a thin layer of indium to weld the MWCNT ends to the opposing substrate.

In this article, the use of MWCNTs as a thermal interface to SiC is explored. Synthesis of MWCNTs with good substrate adhesion was attempted on the Si-face and the C-face of 4H-SiC substrates by a microwave plasma chemical vapor deposition (MPCVD) technique. Once fabricated, the thermal resistances of SiC-MWCNT-Ag interfaces were measured under different pressures and temperatures. The results are compared to those for MWCNT interfaces synthesized on Ti-coated SiC substrates in this study, previous results for MWCNT interfaces on Ti-coated Si substrates [15, 16] and metal foils [17], and other existing thermal interface materials.

EXPERIMENTAL METHODS

Sample Fabrication

An inter-dendritic catalyst templating scheme involving Fe^{3+} ions and an amine-terminated fourth-generation poly(amidoamine) (PAMAM) dendrimer (hereinafter referred to as G4-NH_2) [18] was used to deliver isolated Fe_2O_3 nanoparticles to the C-face and SiO_2(native)/Si-face of 4H-SiC substrates and to Ti (30 nm)-coated surfaces of SiC substrates. The G4-NH_2 dendrimer has an ethylene diamine core and was supplied as a 10% methanol solution from Aldrich (www.aldrich.com). Using a recipe adapted from previous work [19], the catalyst solution was prepared by mixing a 20-mL solution of the G4-NH_2 dendrimer and $FeCl_3 \cdot 6H_2O$ with a G4-NH_2:Fe mole ratio of 1:46. The catalyst was transferred to the substrate surfaces by dip coating for 10 s and calcined at 550°C for 10 min to expose a monolayer of Fe_2O_3 nanoparticles [20].

Microwave plasma chemical vapor deposition (MPCVD) was used to synthesize arrays of vertically oriented MWCNTs from the Fe_2O_3 nanoparticles on SiC and Ti/SiC substrates. Details on the MPCVD system have been presented in previous work [21]. In short, the MPCVD chamber was evacuated to 1 Torr and purged with N_2 for 5 min. To enhance the stability of the Fe_2O_3 nanoparticles, the catalyst was annealed in an N_2 ambient [20]. The growth temperature was 900°C, and the pressure of the reaction chamber was maintained at 10 Torr by flowing 50 SCCM (cubic centimeters per minute at STP) of H_2. Carbon nanotube growth conditions were established by igniting a 200-W plasma and introducing 10 SCCM of CH_4 into the chamber for a duration of 10 min.

Material Characterization

A field-emission scanning electron microscope (FESEM) was used to characterize the morphology and microstructure of the MWCNTs fabricated in this study, and the results are contained in Figure 1. Each synthesized array displayed a general vertical orientation although the tubes are observed to be entangled near their free ends. The arrays ranged in height from 20 to 30 μm. The density of the MWCNT arrays was in the range 10^8–10^9 tubes/mm^2. Figure 1a contains an FESEM image of MWCNTs synthesized on the C-face of SiC. The average diameter of the tubes was approximately 40 nm. Figure 1b contains an image of MWCNTs synthesized on the Si-face of SiC for which the average diameter was approximately 25 nm. Figure 1c contains an image of MWCNTs (average diameter approximately 30 nm) synthesized on Ti-coated SiC. The insets in Figures 1a–c contain images of higher magnification that illustrate profiles characteristic of MWCNTs.

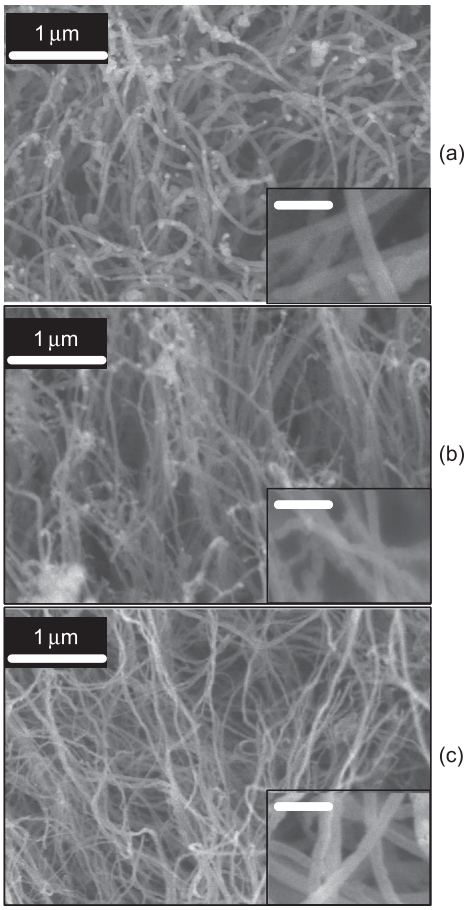

Figure 1. Field-emission scanning electron microscope (FESEM) images of MWCNT arrays fabricated on SiC substrates. (a) Top view of MWCNTs synthesized on the C-face of SiC. The average tube diameter was 40 nm. (b) Tilted view of MWCNTs synthesized on the Si-face of SiC for which the average tube diameter was 25 nm. (c) Tilted view MWCNTs synthesized on Ti-coated SiC. The average tube diameter was 30 nm. The insets (scale bars = 100 nm) are FESEM images of higher magnification.

X-ray photoemission spectroscopy (XPS) was also used to characterize the MWCNT arrays in this study. XPS revealed a high percentage of elemental C (greater than 99%) and little to no Fe near the surface of each MWCNT array. These results, along with corroborating FESEM observations, suggest that synthesis of MWCNTs in this study occurred primarily by a base-growth mechanism [22].

Thermal Characterization

Thermal interface resistance was measured as a function of pressure and temperature using a photoacoustic (PA) technique for which details have been published previously [13]. Briefly, in a given PA measurement the sample surface, which is surrounded by a sealed acoustic cell, is heated by a modulated light source. The amplitude and phase shift of the temperature-induced pressure response in the acoustic chamber is measured by a microphone housed in the chamber wall over a range of laser heating frequencies and can be used with the model of Cola et al. [13] to determine interface resistance. Because of its transient nature, the PA technique can be used to measure multiple internal interface resistances as well as thermal properties within layered materials such as MWCNT array interfaces [13].

In this study, the experimental setup of Cola et al. [13] was modified as illustrated in Figure 2 to allow resistance measurements from room temperature to 250°C (the highest temperature was limited to 250°C to ensure proper operation of the microphone). A heater and thermocouple were embedded near the surface of the sample stage and were connected to a temperature controlling unit. The embedded thermocouple was calibrated to the interface temperature by placing a second thermocouple in the interface of a sample (bare SiC-Ag interface) and recording both thermocouple readings at each tested temperature and pressure. For all experiments, the samples were allowed to dwell at the set temperature for 30 min to ensure steady-state conditions before PA characterization. The rest of the experimental configuration and procedures were identical to those detailed in Cola et al. [13]. Uncertainty in thermal interface resistance ranged from ± 0.5 to 1 mm^2K/W and, as with previous work [13], the uncertainty is dominated by the measurement of the phase shift signal, which exhibited higher noise levels at elevated temperatures as indicated by the larger error bars for higher temperatures in the graphical results that follow.

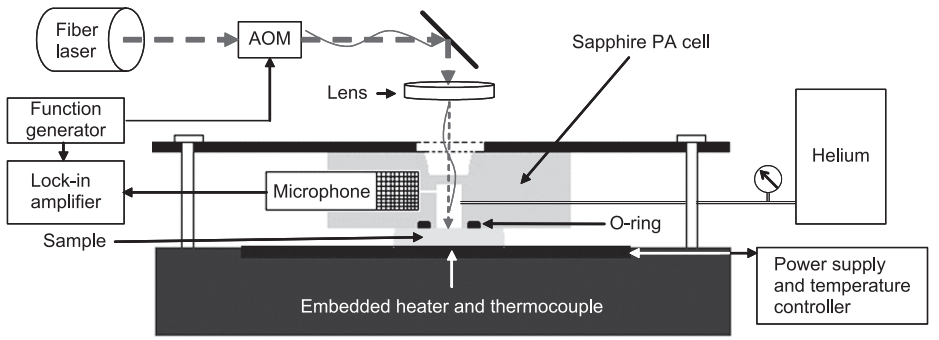

Figure 2. Modified photoacoustic (PA) experimental setup of Cola et al. [13].

RESULTS AND DISCUSSION

The room-temperature (RT) thermal resistances of SiC-MWCNT-Ag interfaces were measured from 69 to 345 kPa using a PA method, and the results are illustrated in Figure 3. The Ag foil (25 μm thick, hard, Premion® Alfa Aesar [www.alfa.com]) was placed atop the MWCNT arrays, and the PA cell was filled with He to control the interface pressure as illustrated in Figure 2. The pressure range was chosen to match common pressures applied between electronic devices and heat sinks. The interfaces with MWCNTs grown on the C-face of SiC achieved resistances as low as 8 mm^2 K/W, yet the resistances of interfaces with MWCNTs grown on the Si-face of SiC were significantly higher. The resistances of the C-face/SiC interfaces are also lower than the resistances of interfaces with MWCNTs grown on Ti-coated SiC substrates.

As contact pressure was increased, the thermal resistances of the C-face/SiC and Ti-coated/SiC interfaces decreased. However, the resistances of the Si-face/SiC interface increased from 69 to 207 kPa before decreasing under continued increases in pressure. This unexpected behavior is likely due to the poor adhesion of the MWCNTs to the Si-face of SiC. Presumably, sufficiently high contact pressure caused the release of some of the MWCNTs from the growth substrate. After testing, the interfaces were separated, and MWCNTs remained well adhered to the C-face of SiC and to the Ti-coated SiC even when subjected to light scratching by tweezers. In contrast, the appearance of the MWCNT arrays grown on the Si-face of SiC was clearly different after testing (some MWCNT material was removed from the substrate upon separation of the interface), and the MWCNTs remaining on the growth substrate could be easily removed from the substrate by light scratching. We postulate that this behavior is the result of favorable chemical bonding in the interface between the C-face/SiC and MWCNTs and between the Ti layer and the MWCNTs where strong Ti-C bonds can form. The reasons for the poorer adhesion between MWCNTs and the Si-face/SiC substrates are not entirely clear and are under continued study.

The thermal resistances at the local interface between the MWCNT free ends and the Ag substrate were determined by the PA technique to be the dominant resistances in the entire interface. Consequently, heat conduction through the

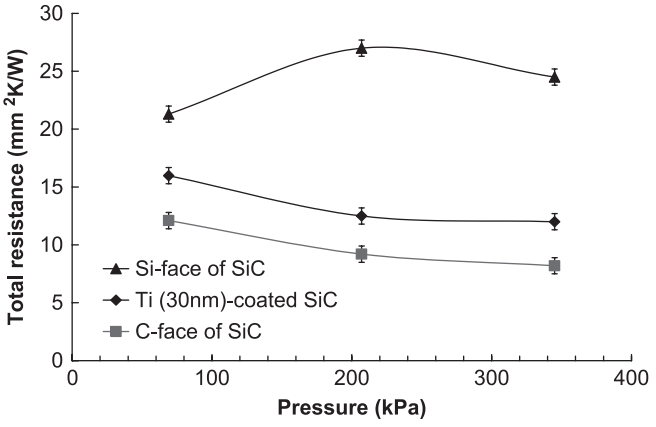

Figure 3. Total thermal resistance as a function of contact pressure for SiC-MWCNT-Ag interfaces at room temperature.

MWCNT array and the associated thermal resistance produces a negligible effect on the measured interface resistances—the room-temperature thermal diffusivities of the MWCNT arrays were measured to be on the order of 10^{-4} m^2/s, which is similar to previous results [13]. Synthesis on the different substrate surfaces studied here produced different array characteristics (e.g., diameter and density) that likely caused the differences in the magnitude of thermal resistances at the interfaces with the free ends of the MWCNTs. Interestingly, the arrays with smaller average tube diameters produced higher thermal resistances, a trend that was also observed in a previous study [16]. The thermal resistances at the interface between the MWCNT arrays and the growth substrates were measured to be approximately 1 mm^2K/W (at each test pressure) for the arrays grown on the C-face of SiC and Ti-coated SiC. However, the resistances at the interface between the MWCNT arrays and the Si-face of SiC growth substrates were measured to be approximately 2 mm^2 K/W at 69 kPa and approximately 5 mm^2 K/W at 207 and 345 kPa, consistent with our observations and postulate of reduced adhesion between the MWCNTs and the Si-face under sufficient contact pressure.

The PA technique was also used to measure the thermal resistances over an elevated temperature range for a MWCNT array interface grown on the C-face of SiC at a contact pressure of 69 kPa. The temperature-dependent thermal properties of SiC were obtained from the literature [23–25], and the resistance of the MWCNT array was lumped into interface resistance when data fitting at elevated temperatures (the required data collection time at each temperature is significantly less in this case, as discussed in a previous study [13]) to reduce the microphone's exposure to such temperatures. The resistances were measured at six different temperatures while heating the interface from RT to 250°C and while cooling the interface from 250°C to RT as illustrated in Figure 4, and the SiC-MWCNT-Ag interface exhibits relatively little temperature dependence in the tested range.

Increasing from room temperature to 100°C causes an increase in resistance for the SiC-MWCNT-Ag interface here that may be the result of evaporation of liquid water menisci, which can decrease contact resistance between nanowires and planar

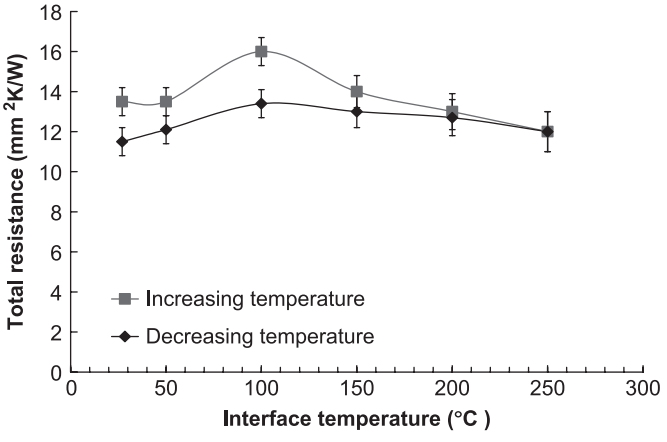

Figure 4. Total thermal resistances as a function of temperature for a C-face-SiC-MWCNT-Ag interface at 69 kPa. The measurements were taken during heating and subsequent cooling of the interface.

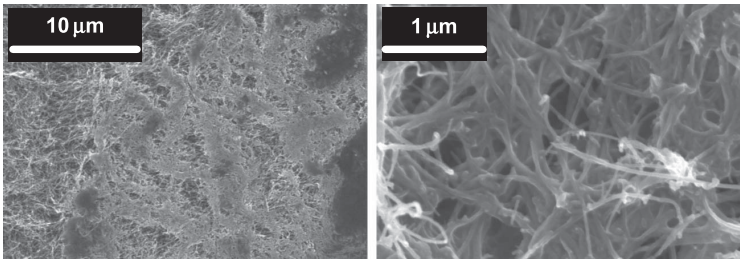

Figure 5. Top view FESEM images of increasing magnification that illustrate the material deposit that was present at the free ends of the MWCNT array after heating the SiC-MWCNT-Ag interface from RT to 250°C and then cooling it back to RT.

substrates [26]. In addition, the characteristic phonon wavelength $\lambda = h\upsilon/k_B T$ in most crystalline solids is on the order of 1 nm at room temperature, where h is the Planck constant and υ is the sound velocity in the material. As temperature increases, the dominant wavelength decreases, causing the likelihood of increased diffuse boundary scattering, which would tend to increase interface resistance for most materials [27, 28].

Above 100°C as temperature increases, a decreasing trend in resistance is observed. Upon attaining the maximum temperature and then systematically cooling the substrate, a hysteresis is observed such that the thermal resistance is less after heating to the maximum temperature of 250°C. After a complete temperature cycle, the interface was reheated to 100°C and the measured thermal resistance (approximately 14 mm^2 K/W) confirmed the hysteretic effects of heating. Notably, when the tested interface was separated after the experiment, the MWCNT free ends were coated with additional material that likely diffused from the Ag surface (see Figure 5). This temperature-induced interface diffusion or reordering presumably created more intimate contact between the MWCNT free ends and the Ag, causing slightly enhanced heat transfer, and such diffusion coating of CNTs at moderate temperatures has been observed previously [29, 30].

In previous studies [15, 16], the thermal resistances of MWCNT interfaces grown on Ti-coated Si substrates have been measured to be as low as 7–8 mm^2 K/W, which is similar to the lowest resistance (8 mm^2 K/W) recorded here for MWCNTs grown on the C-face of SiC. The resistances of interfaces consisting of MWCNTs grown on both sides of metal foil, which have been measured to be as low as 9 mm^2 K/W [17], are also comparable to the resistances of the C-face/SiC-MWCNT-Ag interfaces here. State-of-the-art thermal interface materials such as greases, conductive particle-filled polymers and phase-change waxes, and solder can produce resistances in the range of 5 to 30 mm^2 K/W [31]. However, the MWCNT array interfaces have the unique advantages of being completely dry and removable while achieving thermal resistances at the low end of this range.

CONCLUSIONS

This study has demonstrated that well-bonded MWCNT arrays can be directly synthesized on the C-face of 4H-SiC substrates without the application of an adhesion layer such as Ti and that they achieve thermal interface resistances less than 10 mm^2

K/W. Growth on the Si-face of the SiC substrates was also demonstrated; however, the adhesion of the arrays was poor, and the thermal resistances of the assembled interfaces were significantly higher. The thermal resistances of the SiC-MWCNT-Ag interfaces were measured to compare favorably to state-of-the-art interface materials and exhibit weak temperature dependence from room temperature to 250°C. These characteristics make MWCNT arrays an excellent candidate to address the thermal management needs of high-temperature and high-power SiC devices.

REFERENCES

1. W.Z. Chen, K.Y. Lee and M.A. Capano, Growth and Characterization of Nitrogen-Doped C-Face 4H-SiC Epilayers, *Journal of Crystal Growth*, vol. 297, p. 265, 2006.
2. K.Y. Lee and M.A. Capano, The Correlation of Surface Defects and Reverse Breakdown of 4H-SiC Schottky Barrier Diodes, *Journal of Electronic Materials*, vol. 36, p. 272, 2007.
3. Y. Wang, G.N. Ali, M.K. Mikhov, V. Vaidyanathan, B.J. Skromme, B. Raghothamachar and M. Dudley, Correlation between Morphological Defects, Electron Beam-Induced Current Imaging, and the Electrical Properties of 4H-SiC Schottky Diodes, *Journal of Applied Physics*, vol. 97, p. 013540, 2005.
4. S. Tumakha, D.J. Ewing, L.M. Porter, Q. Wahab, X. Ma, T.S. Sudharshan and L.J. Brillson, Defect-Driven Inhomogeneities in Ni/4H-SiC Schottky Barriers, *Applied Physics Letters*, vol. 87, p. 242106, 2005.
5. Y. Goldberg, M.E. Levinshtein and S.L. Rumyantsev, Chapter 5, in M.E. Levinshtein, S.L. Rumyantsev and M.S. Shur, *Properties of Advanced Semiconductor Materials GaN, AlN, SiC, BN, SiC, SiGe*, pp. 93–148, John Wiley & Sons, Inc., New York, 2001.
6. J.B. Casady and R.W. Johnson, Status of Silicon Carbide (SiC) as a Wide-Bandgap Semiconductor for High-Temperature Applications: A Review, *Solid State Electronics*, vol. 39, pp. 1409–1422, 1996.
7. H.F. Chuang, S.M. Cooper, M. Meyyappan and B.A. Cruden, Improvement of Thermal Contact Resistance by Carbon Nanotubes and Nanofibers, *Journal of Nanoscience and Nanotechnology*, vol. 4, pp. 964–967, 2004.
8. Q. Ngo, B.A. Gurden, A.M. Cassell, M.D. Walker, Q. Ye, J.E. Koehne, M. Meyyappan, J. Li and C.Y. Yang, Thermal Interface Properties of Cu-Filled Vertically Aligned Carbon Nanofiber Arrays, *Nano Letters*, vol. 4, pp. 2403–2407, 2004.
9. J. Xu and T.S. Fisher, Enhanced Thermal Contact Conductance Using Carbon Nanotube Array Interfaces, *IEEE Transactions on Components and Packaging Technologies*, vol. 29, pp. 261–267, 2006.
10. J.X. Hu, A.A. Padilla, J. Xu, T.S. Fisher and K.E. Goodson, 3-Omega Measurements of Vertically Oriented Carbon Nanotubes on Silicon, *ASME Journal of Heat Transfer*, vol. 128, pp. 1109–1113, 2006.
11. X. Wang, Z. Zhong and J. Xu, Noncontact Thermal Characterization of Multiwall Carbon Nanotubes, *Journal of Applied Physics*, vol. 97, p. 064302, 2005.
12. Y. Xu, Y. Zhang, E. Suhir and X. Wang, Thermal Properties of Carbon Nanotube Array Used for Integrated Circuit Cooling, *Journal of Applied Physics*, vol. 100, p. 074302, 2006.
13. B.A. Cola, J. Xu, C. Cheng, H. Hu, X. Xu and T.S. Fisher, Photoacoustic Characterization of Carbon Nanotube Array Thermal Interfaces, *Journal of Applied Physics*, vol. 101, p. 054313, 2007.
14. T. Tong, Y. Zhao, L. Delzeit, A. Kashani, M. Meyyappan and A. Majumdar, Dense Vertically Aligned Multiwalled Carbon Nanotube Arrays as Thermal Interface Materials, *IEEE Transactions on Components and Packaging Technologies*, vol. 30, pp. 92–99, 2007.

15. P.B. Amama, B.A. Cola, T.D. Sands, X. Xu and T.S. Fisher, Dendrimer-Assisted Controlled Growth of Carbon Nanotubes for Enhanced Thermal Interface Conductance, *Nanotechnology*, vol. 18, p. 385303, 2007.
16. B.A. Cola, P.B. Amama, X. Xu and T.S. Fisher, The Effects of Growth Temperature on Carbon Nanotube Array Thermal Interfaces, *ASME Journal of Heat Transfer*, in press.
17. B.A. Cola, X. Xu and T.S. Fisher, Increased Real Contact in Thermal Interfaces: A Carbon Nanotube/Foil Material, *Applied Physics Letters*, vol. 90, p. 093513, 2007.
18. R.W.J. Scott, O.M. Wilson and R.M. Crooks, Synthesis, Characterization, and Applications of Dendrimer-Encapsulated Nanoparticles, *Journal of Physical Chemistry B*., vol. 109, pp. 692–704, 2005.
19. J.K. Vohs, J.J. Brege, J.E. Raymond, A.E. Brown, G.L. William and B.D. Fahlman, Low-Temperature Growth of Carbon Nanotubes from the Catalytic Decomposition of Carbon Tetrachloride, *Journal of the American Chemical Society*, vol. 126, pp. 9936–9937, 2004.
20. P.B. Amama, M.R. Maschmann, T.S. Fisher and T.D. Sands, Dendrimer-Templated Fe Nanoparticles for the Growth of Single-Wall Carbon Nanotubes by Plasma-Enhanced CVD, *Journal of Physical Chemistry B*, vol. 110, pp. 10636–10644, 2006.
21. M.R. Maschmann, P.B. Amama, A. Goyal, Z. Iqbal, R. Gat and T.S. Fisher, Parametric Study of Synthesis Conditions in Plasma-Enhanced CVD of High-Quality Single-Walled Carbon Nanotubes, *Carbon*, vol. 44, pp. 10–18, 2006.
22. M. Terrones, Synthesis, Properties, and Applications of Carbon Nanotubes, *Annual Review of Materials Research*, vol. 33, pp. 419–501, 2003.
23. R.P. Joshi, P.G. Neudeck and C. Fazi, Analysis of the Temperature Dependent Thermal Conductivity of Silicon Carbide for High Temperature Applications, *Journal of Applied Physics*, vol. 88, pp. 265–269, 2000.
24. Y.S. Touloukian, R.W. Powell, C.Y. Ho and P.G. Klemens, *Thermophysical Properties of Matter – Thermal Conductivity Nonmetallic Solids*, pp. 585–588, the TPRC Data Series, vol. 2, 1970.
25. Y.S. Touloukian and E.H. Buyco, *Thermophysical Properties of Matter – Specific Heat Nonmetallic Solids*, pp. 448–449, the TPRC Data Series, vol. 5, 1970.
26. V. Bahadur, J. Xu, Y. Liu and T.S. Fisher, Thermal Resistance of Nanowire-Plane Interfaces, *Journal of Heat Transfer*, vol. 127, pp. 664–668, 2005.
27. R. Yang and G. Chen, Thermal Conductivity Modeling of Periodic Two-Dimensional Nanocomposites, *Physical Review B*, vol. 69, p. 195316, 2004.
28. E.T. Swartz and R.O. Pohl, Thermal Boundary Resistance, *Reviews of Modern Physics*, vol. 61, pp. 605–668, 1989.
29. X. Chen, J. Xia, J. Peng, W. Li and S. Xie, Carbon-Nanotube Metal-Matrix Composites Prepared by Electroless Plating, *Composites Science and Technology*, vol. 60, pp. 301–306, 2000.
30. L. Chen, Y. Zeng, P. Nyugen and T.L. Alford, Silver Diffusion and Defect Formation in Si (111) Substrate at Elevated Temperatures, *Materials Chemistry and Physics*, vol. 76, pp. 224–227, 2002.
31. E.C. Samson, S.V. Machiroutu, J.Y. Chang, I. Santos, J. Hermerding, A. Dani, R. Prasher and D.W. Song, Interface Material Selection and a Thermal Management Technique in Second-Generation Platforms Built on Intel® Centrino™ Mobile Technology, *Intel Technology Journal*, vol. 9, pp. 75–86, 2005.